Chinese Journal of Polymer Science Vol. 34, No. 2, (2016), 135–146

Chinese Journal of Polymer Science

Emulsifier-free Emulsion Polymerized Poly(MMA-HEMA-Eu(AA)$_3$Phen)/Fe_3O_4 Magnetic Fluorescent Bifunctional Nanospheres for Magnetic Resonance and Optical Imaging*

Chen Hu[a†], Tian Xia[b†], Ying Gong[a], Xin Wang[a], Ruan-qing Liu[a], Quan-yuan Zhang[a], Chang-feng Yi[a], Zu-shun Xu[a**] and Ding-zong Guo[b**]

[a] *Hubei Collaborative Innovation Center for Advanced Organic Chemical Materials, Ministry of Education Key Laboratory for The Green Preparation and Application of Functional Material, Hubei University, Wuhan 430062, China*

[b] *College of Veterinary Medicine, Huazhong Agricultural University, Wuhan 430070, China*

Abstract Integration of biocompatibility with superparamagnetic Fe_3O_4 nanoparticles and luminescence rare earth complexes Eu(AA)$_3$Phen was carried out to form bifunctional nanospheres for using in bioimaging applications. The nanospheres Poly(MMA-HEMA-Eu(AA)$_3$Phen)/Fe_3O_4 exhibit magnetic and fluorescent properties that are favorable for the use in drug delivery, magnetic separation and MR imaging for biomedical research. The TEM and SEM studies reveal that the bifunctional nanospheres have core-shell structure, in a spherical shape with a size ranging from 140 nm to 180 nm. In MRI experiments, a clear negative contrast enhancement in T_2 images and the r_2 reaches 568.82 $(mmol \cdot L^{-1})^{-1} \cdot s^{-1}$. *In vivo* magnetic and fluorescence resonance imaging results suggest the nanospheres are able to preferentially accumulate in liver and spleen tissues to allow dual-modal detection of cancer cells in a living body.

Keywords: Magnetic; Fluorescent; Bifunctional nanospheres; MR image.

INTRODUCTION

Magnetic fluorescent nanospheres with characteristics of fluorescent tracer, magnetic responsiveness and surface functionalization have been widely used in the field of biomedical and bioengineering applications, such as cell separation, immobilized enzyme, magnetic resonance and targeted drug[1–3]. So it has been widely investigated, especially in the medical diagnostics and optical imaging[4, 5], and magnetic, fluorescent nanospheres by non-invasive MRI to identify malignant tissue, and through high resolution in the operation of fluorescence imaging provided the information to determine the edge of the tumor cells. The combination of fluorescent and superparamagnetic properties at the nanoscale level in a controlled means can facilitate the biological applications of bifunctional nanoparticles[6], and magnetic, fluorescent microspheres used in biomedicine have many advantages. Recently, researchers have created bifunctional imaging probes with both magnetic and optical imaging modes[7–10]. For example, fluorescent quantum dots (QDs) or organic dyes incorporated into Fe_3O_4 nanoparticles or gadolinium chelates have been produced[6, 11]. For *in vivo* imaging, nanoparticles should possess good colloidal stability and low toxicity in a biological environment[12]. Unfortunately, organic dyes

* This work was financially supported by the National Natural Science Foundation of China (No. 51273058) and in part, by the National Key Technology R&D Program of China (No. 2012BAD12B03).

** Corresponding authors: Zu-shun Xu (徐祖顺), E-mail: zushunxu@hubu.edu.cn
Ding-zong Guo (郭定宗), E-mail: hlgdz@163.com

† These two authors contributed equally to this project.

Received June 17, 2015; Revised August 24, 2015; Accepted September 4, 2015
doi: 10.1007/s10118-016-1739-y

suffer from poor photochemical stability, photo-bleaching, short lifetime and potential toxicity[13], and the heavy metals used in the synthesis of the QDs are toxic[14] consequently hindering their clinical application. However, direct combination of magnetic nanoparticles with luminescent materials usually results in fluorescence quenching due to the Fe_3O_4 particles[15]. To solve this problem, an inert SiO_2 layer has been inserted between the magnetic core and the luminescent materials[16, 17]. However, this method was difficult to control the particle size, and the biocompatibility is not good. An alternative way was inserting a non-luminescent polymer layer between the Fe_3O_4 core and fluorescent polymer shell, which acted as an inert layer to sustain fluorescence, and the direct contact between the magnetic NPs and luminescent polymer was avoided. For example, researchers have reported[18–21] some Fe_3O_4@rare-earth (RE) complex core-shell magnetic fluorescent nanocomposites, during the preparation, high temperature was needed and not convenient to operate. Therefore, due to the relative complexity and modest efficiency of current processes[22], convenient approaches are needed to design and synthesize functional nanostructures. In our previous work[23], we developed a new and facile way to prepare the magnetic fluorescent Fe_3O_4/Poly(St-*co*-GMA) nanoparticles by emulsifier-free emulsion polymerization. The technique has several advantages. (1) The method of seed emulsifier-free emulsion polymerization was very clean, and the produced microspheres without other surfactants can be used directly. (2) The reaction temperature was 75 °C, it was convenient to operate, and oxidation of the modified Fe_3O_4 nanoparticles can be avoid. In the present work, to further endow the polymer nanospheres with additional favorable properties, we chose a functional monomer 2-hydroxyethyl methacrylate (HEMA) and prepared core-shell Poly(MMA-HEMA-$Eu(AA)_3Phen$)/Fe_3O_4 magnetic fluorescent bifunctional nanospheres by emulsifier-free emulsion polymerization. The prepared nanospheres can be used directly after dialysis treatment which avoids the multistep purification processes. In addition, functional hydroxyl groups in the HEMA unit also serve as sites for further surface chemical modification which can impart some other advantages to the nanospheres. The superparamagnetic, luminescent and cytocompatible properties of the microspheres are determined, and *in vivo* MR and optical image are also demonstrated.

MATERIALS AND METHODS

Materials

Europium oxide (Eu_2O_3, 99.99 wt%) was purchased from Shanghai Yuelong Nonferrous Metal and used without further purification. Methyl methacrylate (MMA, 98%) and acrylic acid (AA, 98%) were purified by vacuum distillation prior to use, 2-hydroxyethyl methacrylate (HEMA, 98%) was purchased from Acros Organics and used as received. Potassium peroxodisulfate (KPS) was purified by recrystallization in distilled water and then dried under vacuum. Iron chloride tetrahydrate, ammonium hydroxide ($NH_3{\cdot}H_2O$, 25%–28%), oleic acid (OA), hydrochloric acid and 1,10-phenanthroline (Phen) were purchased from Sinopharm Chemical Reagent Co.Ltd, China. 3-(4,5-Dimenthyl thiazol-2-yi)-2,5-diphenyl tetrazolium bromide (MTT) was purchased from Sigma-Aldrich.

Preparation of $Eu(AA)_3Phen$, Oleic Acid and NaUA Modified Fe_3O_4 Nanoparticles (OA/NaUA)-Fe_3O_4

The $Eu(AA)_3Phen$, oleic acid and NaUA modified Fe_3O_4 nanoparticles were prepared according to a method described in our previous paper[23, 24]. The modified Fe_3O_4 nanoparticles (OA/NaUA)-Fe_3O_4 were prepared by two steps. The first step was to prepare OA/Fe_3O_4 nanoparticles. 26.115 g $FeCl_3{\cdot}6H_2O$ and 13.31 g $FeCl_2{\cdot}4H_2O$ mixed in 80 mL of deoxygenated water were put into a 250 mL three-necked flask, and 70 mL of $NH_3{\cdot}H_2O$ was added to produce black precipitates. The mixture was heated to 75 °C for 1 h and the product Fe_3O_4 nanoparticles were washed with deoxygenated water for several times, in order to remove the excess $NH_3{\cdot}H_2O$ until a pH value of 7. Next, Fe_3O_4 nanoparticles were dispersed in a 250 mL three-necked flask with a mixture of 50 mL ethanol and 50 mL distilled water under nitrogen with vigorous stirring, 5 g oleic acid was added and heated to 80 °C for 1 h, so OA/Fe_3O_4 nanoparticles were produced. The second step was to produce OA/NaUA modified Fe_3O_4 nanoparticles, after the product OA/Fe_3O_4 nanoparticles were cooled to room temperature, OA/Fe_3O_4 nanoparticles were washed with ethanol three times and dispersed in 25 mL $CHCl_3$, the mixture was added into a 150 mL three-necked flask with 50 mL aqueous solution containing 8 g NaUA. The mixture was

stirred at room temperature for 1 h. The final product OA/NaUA modified Fe_3O_4 nanoparticles were under stirring at room temperature until the weight became constant. (OA/NaUA)-Fe_3O_4 magnetic fluid with a solid of 11.5% was obtained.

Preparation of Magnetic Fluorescent Bifunctonal Nanospheres

The magnetic fluorescent bifunctional nanospheres were prepared by two steps. In the first step, certain amounts of (OA/NaUA)-Fe_3O_4 NPs, MMA, HEMA, and distilled water (recipe given in Table 1) were added to a 250 mL round-bottomed flask equipped with a condenser and stirred under nitrogen atmosphere, a homogeneous solution was obtained. The solution was heated to 75 °C in a water bath, then polymerization was initiated by adding an aqueous solution (5 mL) containing KPS. After 30 min, the primary seeds of Poly(MMA-HEMA)/Fe_3O_4 were produced. In the second step, the $Eu(AA)_3Phen$ was dissolved in 15 mL of distilled water and dropwise added to the mixture for 30 min. After complete addition, the mixture was allowed to polymerize for 4 h at a stirring speed of 360 r/min. All the samples were purified by dialysis against distill water for one week and the distilled water were changed for fresh every 12 h. The solid samples were obtained by dropping the latex into a saturated calcium chloride/methanol solution. The precipitates were purified by washing with distilled water several times and then collected by centrifugation at 4000 r/min. The product were dried at 40 °C in vacuum for 2 days and stored for later measurements.

Table 1. Feed composition of nanospheres

Sample code	MMA (g)	HEMA (g)	$Eu(AA)_3Phen$ (g)	Magnetic fluid (g)	KPS (g)	H_2O (mL)
1	2.50	0.30	0.08	1.44	0.07	50
2	2.50	0.30	0.08	2.88	0.07	50
3	2.50	0.30	0.08	4.30	0.07	50
4	2.50	0.30	0.08	5.60	0.07	50

Determination of Iron Content in Nanosphere Solutions

The weight percentage of iron in the dialyzed nanospheres was measured by inductively coupled plasma atomic emission spectrometry (ICP-AES, optimal 8000, TA, USA). The sample 4 was produced as follows. 1 mL of nanospheres and 10 mL of nitric acid were added into a 100 mL round-bottomed flask, the mixture was heated to 110 °C until the nanospheres completely dissolved, then it was diluted to 50 mL by adding distilled water, shook well and transferred to a centrifuge tube for measurements. The iron content in the nanospheres was determined at the specific Fe absorption wavelength of 248.3 nm.

In vitro Cytotoxicity Test

Most authors have analyzed the effect of SPIONs on cell proliferation and viability by MTT (3-[4,5-dimethylthia-zol-2-yl]-2,5-diphenyl tetrazolinum bromide) assays[25, 26, 27]. So the *in vitro* cytotoxicity of the nanospheres was studied using human HEK293T cell lines by means of a methyl thiazolyl tetrazolium (MTT) assay. The cells are plated on 96-well plates at a density of 1×10^4/well, grown for 24 h at 37 °C and 5% CO_2 in DMEM medium, washed with PBS (pH = 7.4) and incubated with different concentrations of nanosphere solutions (dose diluted by complete medium, 77.5–1240 ug·mL^{-1}) for another 24 h. Afterwards, the supernatants were removed and cells were washed with PBS for several times. MTT solution (10 μL·well^{-1}) was added into each well and incubated for 4 h, the culture medium was discarded. In each well the supernatant was replaced with 150 μL dimethyl sulfoxide (DMSO) to dissolve the crystals by agitation for 10 min. The survived cells converted MTT to formazan, which generated a blue-purple color when dissolved in dimethyl sulfoxide (DMSO). The intensity of formazan was measured at a wavelength of 570 nm using a plate reader for enzyme-linked immunosorbent (ELISA) assays. The following formula was used to calculate the relative cell viability: Relative cell viability (%) = $(OD_{treat}–OD_{background})/(OD_{control}–OD_{bcakground}) \times 100\%$, OD_{treat} from the cells treated with nanospheres, $OD_{control}$ from the cells treated without nanospheres, $OD_{background}$ from the empty cells.

In vivo T_2 MR Image Measurements

An SD mouse with 250 g was used to study the *in vivo* T_2 MR images measurement and T_2 MR images were taken by using the 3T MR scanner. The mouse was anesthetized by 10% chloral hydrate (dosage of 3 mL·kg^{-1}

body weight) and the MRI solution of sample 4 was injected into the mouse through tail vein, the injection dose was 5 mg Fe/kg body weight. The mouse was scanned before and after the administration of sample 4, and the images were got at different time (10 min, 30 min, 1 h, 2 h and 10 h after injection the nanospheres solution). The animals were treated according to the protocols of the Institutional Animal Care and Use Committee at HuBei University as approved by the Institutional Animal Care.

Histological Analysis and Optical Imaging

The mice were sacrificed 10 h after injection with the nanospheres solution. The 4 organ parts liver, spleen, kidney, and lung were fixed in 4% paraformaldehyde for 24 h and transferred to 30% sucrose in the PBS buffer. The tissues were prepared by Prussian blue staining for histological analysis. For luminescence *in vivo* analysis, the images of confocal laser scanning microscopy (CLSM) were obtained from the slides of liver and spleen.

Characterization of the Nanospheres

The surface of the functionalized nanospheres and OA/NaUA modified Fe_3O_4 were confirmed by Fourier transform infrared spectroscopy (FTIR) performed on a Perkin Elmer Spectrum one Transform Infrared spectrometer (USA), the samples were pressed with KBr into compact pellets. The size and the morphology of the particles were examined by using a transmission electron microscope (TEM, Tecnai G20, FEI Corp, USA). The samples were prepared by dropping a dilute solution of nanospheres on the surface of a copper grid and dried at room temperature. The scanning electron microscopy (SEM) images were obtained on a scanning electron microscope (JSM6510LV, JEOL, Japan). The samples were prepared by dropping the diluted nanospheres solution onto glass slides and dried at room temperature. The glass slides were coated with a thin gold film under vacuum. The hydrodynamic diameters of nanospheres in water were measured by dynamic light scattering (DLS, HPPS5001, Malvern Instrument). The structure of the nanospheres and OA/NaUA modified Fe_3O_4 nanoparticles were characterized by X-ray diffraction (X'Pert, Philips Corp. Nederland) using a CuKα radiation source (λ = 0.15418 nm) at a scanning rate of 5 (°)·min^{-1}. The magnetic properties of the OA modified Fe_3O_4 nanoparticles, OA/NaUA modified Fe_3O_4 nanoparticles and functionalized nanospheres were measured by a vibrating sample magnetometer (VSM, HH-15, China). The thermogravimetric analysis (TGA) of the dried powder samples was performed on a Perkin-Elmer TGA-7 instrument from room temperature to 750 °C at a heating rate of 10 K·min^{-1}. The fluorescent properties of nanospheres were investigated by a Hitachi Fluorescence spectrophotometer F-2500 (Hitachi High Technologies Corporation, Japan). The R_2 images measure and *in vivo* MRI experiments were carried out at 25 °C on a 3.0 T whole-body MR scanner (MAGNETOM Trio, A Tim System 3.0 T, Siemens, Munich, Germany), in combination with a wrist joint coil. In the *in vitro* MRI experiments, the parameters were as follows: field of view (FOV) = 120 mm, slice thickness = 2.0 mm, base resolution = 384 × 384, multiple echo times (TE) = 40, 80, 120, 160, 200, 240 and 280 ms, repetition time (TR) = 2890 ms and scanning time = 13–14 min. In the *in vivo* MRI experiments, the field of view (FOV) was 100 mm, base resolution was 192 × 192, slice thickness was 2.0 mm, multiple echo time (TE) was 62 ms, repetition time (TR) was 2890 ms, and flip angle was 120°. The CLSM images of the slices were obtained on a Spectra Physics MaiTai HP tunable 2-photon (690–1040 nm) laser confocal microscope (Carl Zeiss LSM710).

RESULTS AND DISCUSSION

Chemical Structure and Morphology

For OA/NaUA modified Fe_3O_4 nanoparticles the 575 cm^{-1} peak belongs to Fe_3O_4 Fe—O absorption, the peaks at 1624 cm^{-1}, 2921 cm^{-1} and 2851 cm^{-1} are attributed to NaUA as C=C vibration, —CH_2 streching vibration of asymmetry and symmetry, showing the Fe_3O_4 nanoparticles have been successfully modified. In nanospheres the 540 cm^{-1} and 444 cm^{-1} peaks belong to the Fe—O absorption of Fe_3O_4 particles, the peak at 3420 cm^{-1} belongs to the vibration of —OH group in HEAM, the 1734 cm^{-1} peak is attributed to C=O stretching vibration of ester base, and Fig. 1 does not show the characteristic C=C absorption peak of monomer, which means the polymerization is complete.

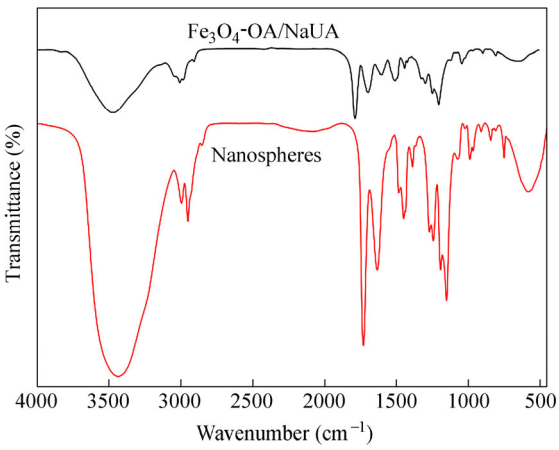

Fig. 1 FTIR spectra of OA/NaUA modified Fe_3O_4 nanoparticles and nanospheres

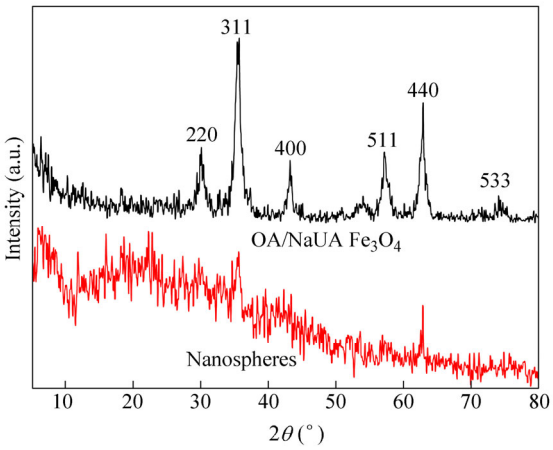

Fig. 2 XRD patterns of OA/NaUA modified Fe_3O_4 nanoparticles and nanospheres

XRD was conducted to identify the crystalline structure of the samples. Figure 2 indicated the XRD patterns of the OA/NaUA modified Fe_3O_4 nanoparticles and nanospheres. As shown in the picture, the OA and NaUA modified Fe_3O_4 nanoparticles yield the main peaks at 2θ of 30.5°, 35.8°, 43.3°, 57.4°, 62.5°, 74.5°, corresponding to the reflection plane indices of (220), (311), (400), (511), (440) and (533). Peak matching with reference inorganic crystal structure database (ICSD) improves that the particles have the cubic Fe_3O_4 crystal structure[28]. The pattern of the nanospheres was consistent with that of the Fe_3O_4 nanoparticles, indicating that a part of the modified Fe_3O_4 nanoparticles were encapsulated forming nanospheres. TEM and SEM were employed to examine the microstructures and morphologies of the nanospheres. The TEM images in Fig. 3 show that the as-prepared nanospheres are monodisperse with a narrow size distribution (see the picture in supporting information), which reveal that almost all the core-shell nanospheres have incorporated modified Fe_3O_4 nanoparticles in the cores. A crucial aspect for many applications of nanospheres is the ability to control their size and, in particular, the size homogeneity. The SEM image Fig. 3(d) shows that the as-prepared nanospheres are about 150 nm in diameter.

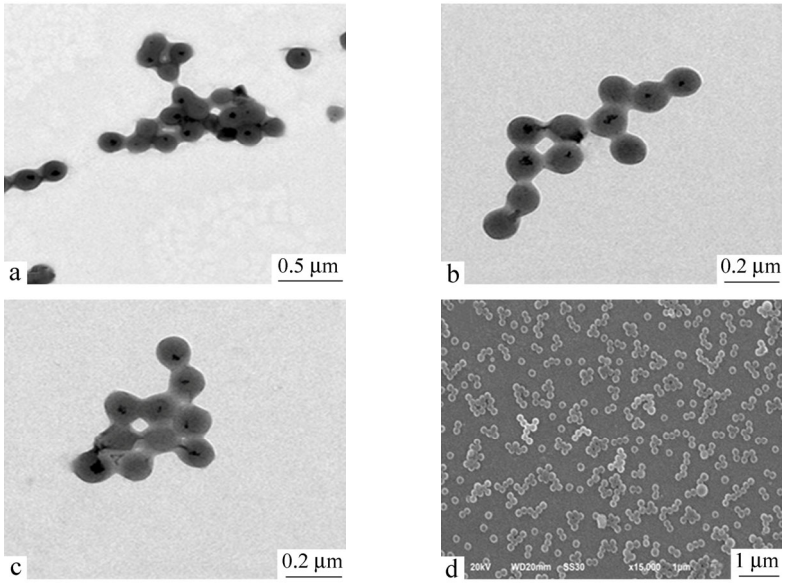

Fig. 3 TEM images of (a) sample 2, (b) sample 3, (c) sample 4 and SEM image of (d) sample 1

Average particle sizes of the nanospheres were examined by dynamic light scattering particle size measuring instrument (DLS). Taking a small amount of dialysis emulsion diluted with distill water and adding into a cuvette, all the samples were under the condition of 25 °C for testing. Figure 4 shows the hydrodynamic diameter of samples 1, 2, 3 and 4. As shown in the picture, all the samples present a narrow particle size distribution, with a size ranging from 140 nm to 180 nm, indicating the soap-free emulsion polymerization preparation has a uniform size of nanospheres which can facilitate their application in biomedical field effectively.

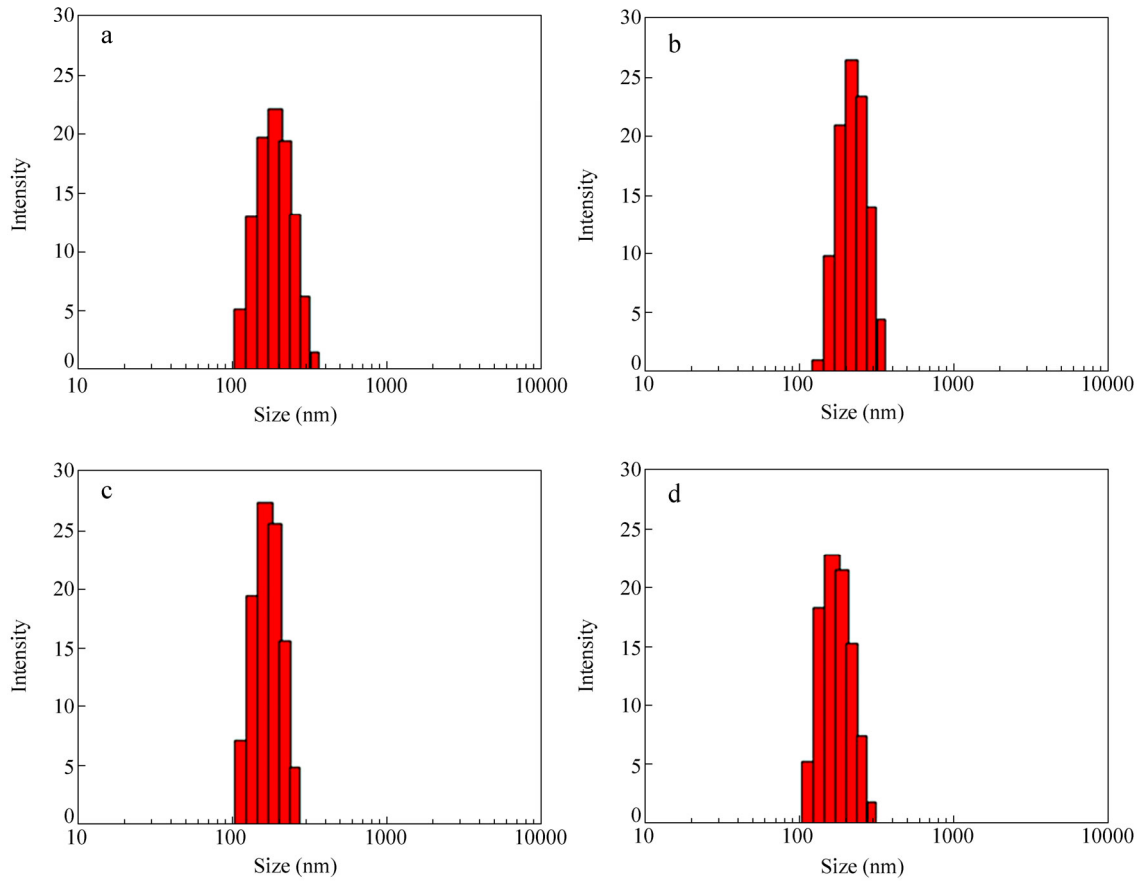

Fig. 4 Hydrodynamic diameter and size distribution of (a) sample 1, (b) sample 2, (c) sample 3 and (d) sample 4

Thermal gravimetric (TG) analysis was performed on samples in nitrogen atmosphere. The TG curve of OA/NaUA modified Fe_3O_4 nanoparticles in Fig. 5 reveals two steps decay. The first stage is indicated by a weight loss of 15% between 30 °C and 450 °C duo to the loss of OA molecules physically adsorbed on the Fe_3O_4 particle surface. The second stage of weight loss of about 61.8% in the range of 450 °C to 750 °C is related to the degradation of NaUA bonded to the Fe_3O_4 particles in the inner layer. The residual weight percentage of samples 2, 3 and 4 at 750 °C is 18.54%, 20.54% and 26.37%, respectively. The remaining materials are mainly rare earth Eu and Fe_3O_4 nanoparticles. The result reveals the nanospheres have excellent thermal property.

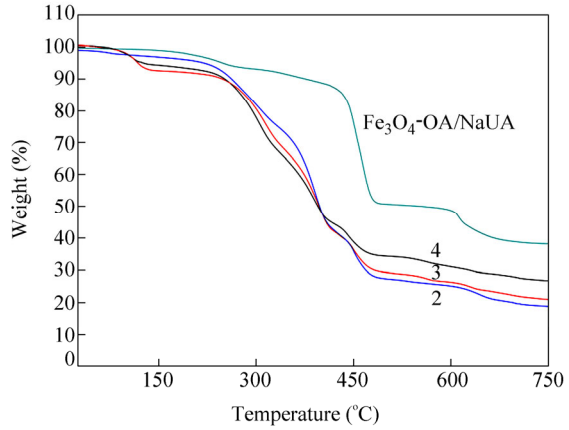

Fig. 5 TG curves of OA/NaUA modified Fe_3O_4 nanoparticles and samples 2, 3 and 4

Magnetic Properties

In order to study the magnetic properties of the nanospheres, the nanosphere samples were tested on a vibrating sample magnetometer at room temperature. As shown in Fig. 6, the samples exhibit superparamagetism with negligible coercivity and remnant magnetization. The saturation magnetization of the OA/NaUA modified Fe_3O_4 nanoparticles and samples 2 and 4 is 17.84 emu·g^{-1}, 1.98 emu·g^{-1} and 2.85 emu·g^{-1}. The loss of saturation magnetization of the samples compared to modified Fe_3O_4 nanoparticles is due to the presence of the non-magnetic polymer which reduces the total magnetization.

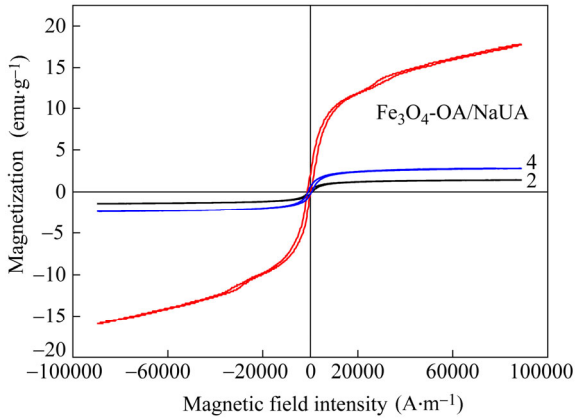

Fig. 6 Room temperature magnetization curves of OA/NaUA modified Fe_3O_4 nanoparticles and samples 2 and 4

Photoluminescence Properties

The excitation and emission spectra of the nanocomposites were tested after being dispersed in water at 0.25 mg·mL^{-1}. In Fig. 7(a), the excitation spectrum consists of two relatively broad peaks with a maximum at 277 nm and a shoulder at 317 nm. The emission spectrum was obtained under excitation of 277 nm. As shown in Fig. 7(b), two peaks at 595 nm and 619 nm appeared as the europium ion (Eu^{3+}) characteristic fluorescence peaks, which can be attributed to $^5D_0 \rightarrow {}^7F_1$ magnetic dipole transition peak and $^5D_0 \rightarrow {}^7F_2$ forced electric dipole transition peak of Eu^{3+} ions, respectively. The most intense peak at 619 nm corresponds to the $^5D_0 \rightarrow {}^7F_2$ transition of the Eu^{3+} ions, as is typically observed, showing the Eu^{3+} ion in the fluorescent magnetic nanospheres. To further study the potential of the nanospheres used as fluorescence labels, the fluorescence intensities from liver and spleen are monitored *in vivo* to confirm accumulation of nanospheres. Seen from Fig. 8, there is no any fluorescence dots observed from the liver (Fig. 8c) and spleen (Fig. 8d) without injection the nanospheres solution. On the contrary, the vivid red fluorescence dots are observed from slices of the liver

(Fig. 8a) and spleen (Fig. 8b) after injection with nanospheres solution. The integration of the superparamagnetic and fluorescence properties in the prepared nanospheres, makes them more attractively be used as dual-modality optical/MRI probes for diagnosing of cancer cells in liver and spleen in clinical applications.

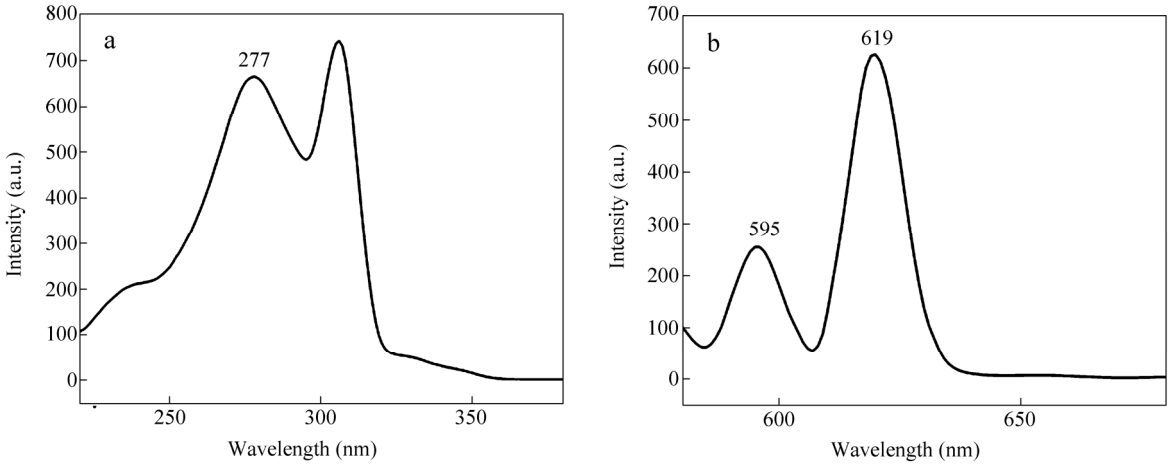

Fig. 7 (a) Excitation spectra of nanospheres (λ = 619 nm); (b) Emission spectra of nanospheres (λ = 277 nm)

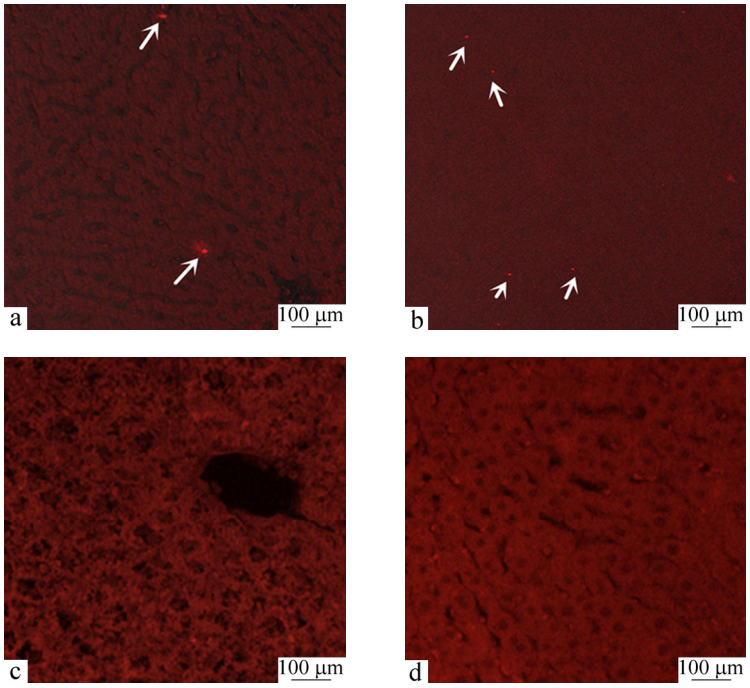

Fig. 8 CLSM images of tissue slices: (a) liver slice and (b) spleen slice after injection with nanospheres solution; (c) liver slice and (d) spleen slice without injection nanospheres solution

Cell Viability

In order to make sure the biocompatibility of nanospheres as biological imaging probe or contrast agent, an MTT assay was employed to test the biocompatibility of the nanospheres. As shown in Fig. 9, the nanospheres exhibit good cytocompatibility with HEK293T cells. Even the concentration of the nanospheres reached 1240 ug·mL^{-1} the cells viability were still over 85%, indicating its large clinical potential. The result clearly indicates that our synthesized nanospheres have low cytotoxicity[29].

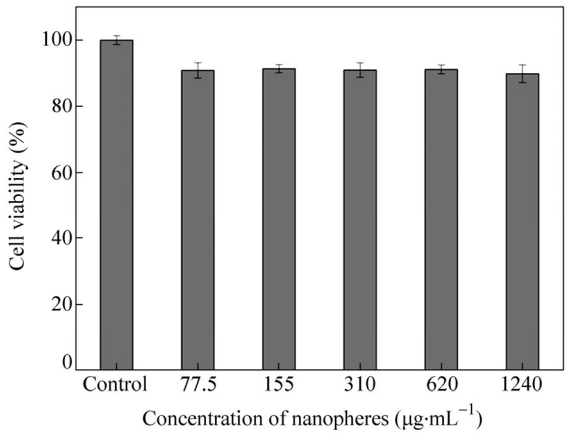

Fig. 9 Cell viability test of HEK293T cells with different concentrations of nanospheres

R_2 Map Images Measure and R_2 Relaxivity

We recorded the *in vitro* T_2-weighted phantom images of 10 different concentrations (0, 0.010, 0.015, 0.020, 0.025, 0.030, 0.035, 0.040, 0.045, 0.050 (Fe) mmol·L^{-1}). Owing to superparamagnetic nature of our nanospheres, the nanospheres can be used as T_2-weigthed contrast agent and shorten the transverse relaxation time (T_2). The T_2-weighted MR images were acquired on a 3.0 T MR scanner revealing the concentration-dependent darkening effect. Figure 10 indicates negative contrast enhancement by the nanospheres, which implies that these nanospheres have potential as contrast agents in MR imaging. Due to the Fe concentration of the nanospheres increase, the generated MR contrast signal intensity lead to a proportional decrease (darken of the images), the shortening of T_2 by the embedded modified Fe_3O_4 nanoparticles. The respective R_2 relaxivities are estimated from the slope in the plots of $1/T_2$ versus Fe concentration. The $1/T_2$ is calculated to be 568.82 (mmol·L^{-1})$^{-1}$·s^{-1}, and that means the nanospheres have a great potential to be used as T_2 contrast agent in biomedical applications in the future.

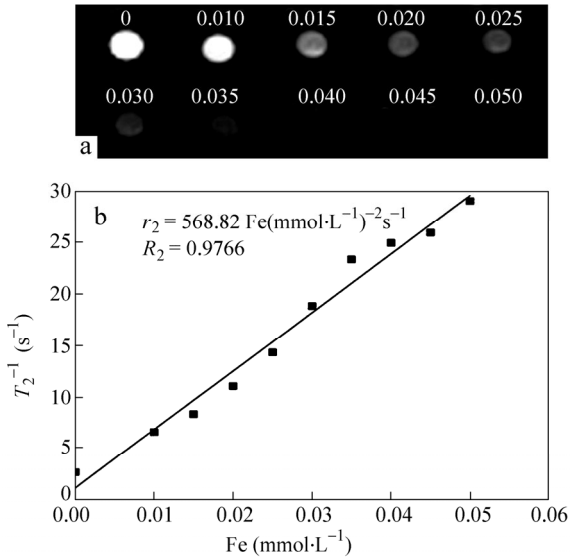

Fig. 10 (a) The MR signal intensity change according to the Fe concentration of nanospheres; (b) Relaxation rate ($1/T_2$, S^{-1}) as a function of Fe concentration (mmol·L^{-1}) of nanospheres solution

In vivo T_2 MR Images Experiment

Many imaging contrast agents have been incorporated into multifunctional nanocarriers, including fluorescence optical imaging, magnetic resonance imaging (MRI), positron-emission tomography (PET) and computed

tomography (CT)[30]. Among MRI contrast agents, superparamagnetic iron oxide is a nanoscale MRI T_2 contrast agent with biocompatibility and high sensitivity[31]. The difference between human body organizations, the normal and pathological changes of the organization of the tissue hydrogen nuclear density, relaxation time T_1, T_2 are the three basic parameters of MRI used in clinical diagosis. MRI is currently one of the most powerful diagnosis tools in medical science and basic research fields[32]. The images acquired by MRI are very clear, improving the efficiency of the doctors′ diagnosis greatly and avoiding the caesarean section of thoracic abdominal diagnosis. As MRI does not use X-ray to hurt human body and also the radiography agent that causes allergic reaction, so it is safe. Iron oxide nanoparticles (usually Fe_3O_4 nanoparticles) have become extremely popular due to their ability to dramatically shorten T_2^* relaxation times in the liver and spleen, by selective uptake of the reticuloendotherial system (RES). The capability of the nanospheres as multimodal imaging probes was further evidenced *in vivo*[33]. To examine the possibility of using magnetic fluorescent nanospheres as an MRI contrast agent, we measured relaxation times at a 3.0 T human clinical scanner of the size-tuned nanoparticles. The magnetic fluorescent nanospheres can clearly decrease the transverse relaxation time (T_2). MRI contrast agents can help to clarify images and to allow better interpretation[34]. For *in vivo* MR imaging, 5 mg Fe per kg of mouse body weight were injected (rapid single shot) into a mouse through its tail vein, T_2-weighted MR imaging was conducted after intravenous injection of the nanosphere solution. The degree of the T_2 contrast effect is typically represented by the spin-spin R_2 relaxivity ($R_2 = 1/T_2$), where higher values of R_2 result in a stronger contrast effect. The relaxivity coefficient r_2, which is obtained as the gradient of the plot of R_2 versus the molarity of magnetic atoms, is a standardized contrast enhancement indicator[35]. Strong signals from the liver and spleen sites were observed 10 min after injection, suggesting high liver and spleen uptake of nanospheres. Figure 11(a) shows obvious darkening effects in the liver and spleen after injection, and the biggest reduction of the relative of MRI signal in the liver and spleen reaches 94.8% at 10 min and 95.5% at 2 h after injection (observed from Fig. 11b), the imaging effect can last for 10 h.

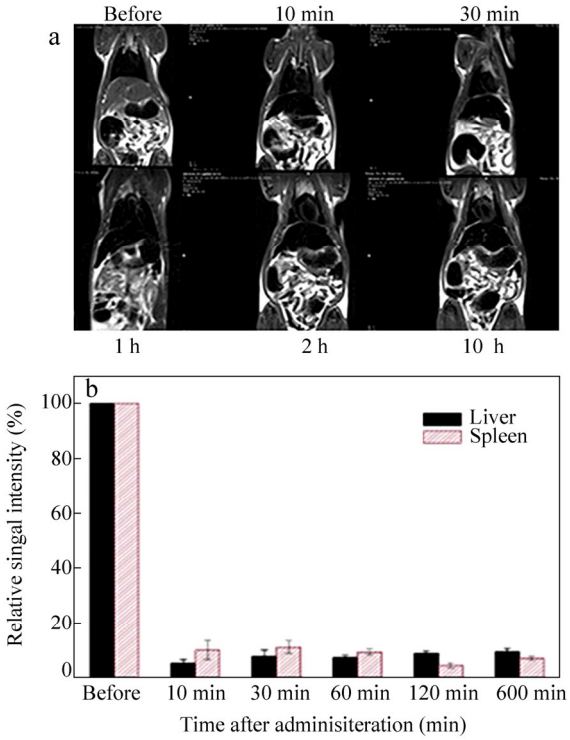

Fig. 11 (a) T_2-weigthed MR images of mouse acquired before and at different time after injection the nanosphere solution; (b) Relative MRI signal intensity of mouse liver and spleen acquired before and after injection the nanophere solution

In order to further confirm the accumulation of nanospheres in the mice, we took tissue slices from 4 different parts of the body, respectively which were liver, spleen, kidney, and lung, 10 h after injection and stained with Prussian blue. Seen from Fig. 12, the blue dots were most existed in liver and spleen, and in kidney and lung there were no any blue dots. The result indicates the nanospheres are mainly concentrated in the liver and spleen, so the nanospheres can be served as negative (T_2) MR contrast agents in these two organs.

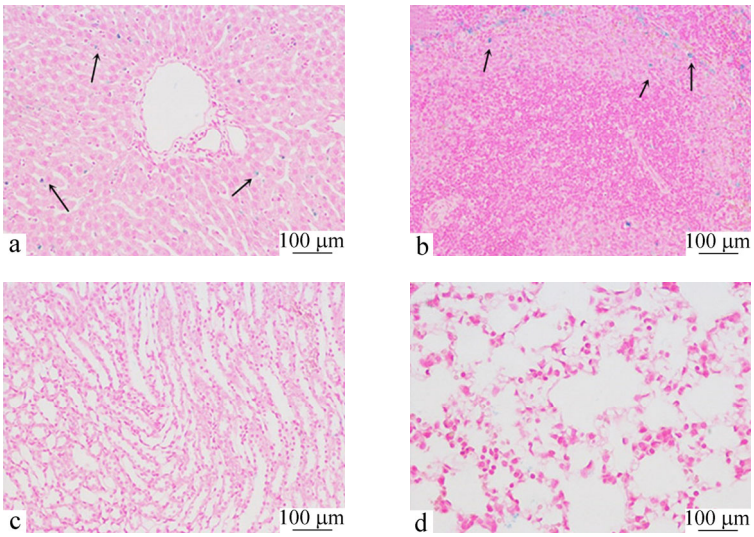

Fig. 12 Prussian blue staining images of (a) liver, (b) spleen, (c) kidney and (d) lung tissue slices excised from mice 10 h after tail vein injection of nanosphere solution

CONCLUSIONS

In summary, a modified approach was used to synthesize highly water-dispersible magnetite fluid with uniform size by modifying with OA and NaUA. More importantly, the nanospheres not only have excellent superparamagnetism, exhibit fluorescent and dispersing stability, but also show low cytotoxicity, and good biocompatibility, which makes them promising candidates for applications in various bio-related fields, such as MRI contrast agents and optical imaging. This work demonstrates the potential of nanosphere based dual-modal nanoprobes for versatile *in vitro* and *in vivo* clinical applications in future.

REFERENCES

1 Gao, Y., Zou, X., Zhao, J.X.J., Li, Y. and Su, X.G., Colloid Surface B., 2013, 112: 128
2 Ou, J., Wang, F., Huang, Y.J., Li, D.S., Jiang, Y.M., Qin, Q.H., Stachurski, Z.H., Tricoli, A. and Zhang, T.N., Colloid Surface B., 2014, 117: 466
3 Wang, H., Maraenko, A., Cao, G.X., Gai, Z., Hong, K.L., Banerjee, P. and Zhou, S.Q., ACS Appl. Mater. Interfaces, 2014, 6: 15309
4 Chen, Y., Chen, H.R., Zhang, S.J., Chen, F., Zhang, L.X., Zhang, J.M., Zhu, M., Wu, H.X., Guo, L.M., Feng, J.W. and Shi, J.L., Adv. Funct. Mater., 2011, 21: 270
5 Li, K., Ding, D., Huo, D., Pu, K.Y., Thao, N.N.P., Hu, Y., Li, Z. and Liu, B., Adv. Funct. Mater., 2012, 22: 3107
6 Lee, C.S., Chang, H.H., Bea, P.K., Jung, J. and Chung, B.H., Macromol. Biosci., 2013, 13: 321
7 Mulder, W.J., Griffioen, A.W., Strijkers, G.J., Cormode, D.P., Nicolay, K. and Fayad, Z.A., Adv. Nanomedicine, 2007, 2: 307
8 Yang, H., Santra, S., Walter, G.A. and Holloway, P.H., Adv. Mater., 2006, 18: 2890

9 Yi, D.K., Selvan, S.T., Lee, S.S., Papaefthymiou, G.C., Kundaliya, D. and Ying, J.Y., J. Am. Chem. Soc., 2005, 127: 4990
10 Tan, W.B. and Zhang, Y., Adv. Mater., 2005, 17: 2375
11 Caravan, P., Ellison, J.J., McMurry, T.J. and Lauffer, R.B., Chem. Rev., 1999, 99: 2293
12 Na, H.B., Song, I.C. and Hyeon, T., Adv. Mater., 2009, 21: 2133
13 Ma, Z.Y., Dosev, D., Nichkova, M., Gee, S.J., Hammock, B.D. and Kennedy, I.M., J. Mater Chem., 2009, 19: 4695
14 Kievit, F.M. and Zhang, M., Adv. Mater., 2011, 23: H217
15 Levin, C.S., Hofmann, C., Ali, T.A., Kelly, A.T., Morosan, E., Nordlander, P., Whitmire, K.H. and Halas, N.J., ACS Nano., 2009, 3: 1379
16 Gai, S.L., Yang, P.P., Li, C.X., Wang, W.X., Dai, Y.L., Niu, N. and Lin, J., Adv. Funct. Mater., 2010, 20: 1166
17 Tong, L., Shi, J., Liu, D., Li, Q., Ren, X. and Yang, H., J. Phys. Chem. C, 2012, 116: 7153
18 Lu, P., Zhang, J.L., Liu, Y.L., Sun, D.H., Liu, G.X., Hong, G.Y. and Ni, J.Z., Talanta, 2010, 82: 450
19 Peng, H.X., Liu, G.X., Dong, X.T., Wang, J.X., Xu, J. and Yu, W.S., J. Alloys Compd., 2011, 509: 6930
20 Wang, W., Zou, M. and Chen, K.Z., Chem. Commun., 2010, 46: 5100
21 Feng, J., Song, S.Y., Deng, R.P., Fan, W.Q. and Zhang, H.J., Langmuir, 2010, 26: 3596
22 Gupta, A.K. and Gupta, M., Biomaterials, 2005, 26: 3995
23 Zhu, H.E., Shang, Y.L., Wang, W.H., Zhou, Y.J., Li, P.H., Yan, K., Wu, S.L., Yeung, K.W.K., Xu, Z.S., Xu, H.B. and Chu, P.K., Small, 2013, 9: 2991
24 Hu, X.X., Li, P.H., Yeung, K.W.K., Chu, P.K., Wu, S.L. and Xu, Z.S., J. Polym. Sci., Part A: Polym. Chem., 2004, 42: 5961
25 Arbab, A.S., Bashaw, L.A., Miller, B.R., Jordan, E.K., Bulte, J.W. and Frank, J.A., Transplantation, 2003, 76: 1123
26 Arbab, A.S., Yocum, G.T., Kalish, H., Jordan, E.K., Anderson, S.A., Khakoo, A.Y., Read, E.J. and Frank, J.A., Blood, 2004, 104: 1217
27 Hsiao, J.K., Tai, M.F., Chu, H.H., Chen, S.T., Li, H., Lai, D.M., Hsieh, S.T., Wang, J.L. and Liu, H.M., Magn. Reson. Med., 2007, 58: 717
28 Li, X.L., Li, H., Liu, G.Q., Deng, Z.W., Wu, S.L., Li, H.P., Xu, Z.S., Xu, H.B. and Chu, P.K., Biomaterials, 2012, 33: 3013
29 Babincova, M., Sourvong, P., Leszczynska, D. and Babinec, P., Medical Hypotheses, 2000, 55: 459
30 Zhang, Y., Wang, X., Guo, M. and Wang, C., Chinese J. Polym. Sci., 2014, 32(10): 1329
31 Gong, F.M., Zhang, Z.Q., Chen, X.D., Zhang, L., Yu, X.S., Yang, Q.H., Shuai, X.T., Liang, B.L. and Cheng, D., Chinese J. Polym. Sci., 2014, 32(3): 321
32 Brown, M.A. and Semelka, R.C., “MRI: Basic principles and applications”, Wiley, New York, 2003
33 Cheng, L., Yang, K., Li, Y.G., Chen, J.H., Wang, C., Shao, M.W., Lee, S.T. and Liu, Z., Angew. Chem. Int. Ed., 2011, 50: 7385
34 Na, H.B., Song, I.C. and Hyeon, T., Adv. Mater., 2009, 21: 2133
35 Hao, B.R., Xing, R.J., Xu, Z.C., Hou, Y.L., Gao, S. and Sun, S.H., Adv. Mater., 2010, 22: 2729